



79-11-73

EUROPEAN ORGANIZATION FOR NUCLEAR RESEARCH

CERN-EP/79-89
DD/79-05
14 August 1979

MULTIPLEXED FOCUSING ČERENKOV COUNTER

M. Benot and R. Meunier^{*)}

CERN, Geneva, Switzerland

ABSTRACT

An optical system replacing the usual diaphragm is described, which can extend the angular and velocity acceptance of focusing Čerenkov counters. The use of such counters is therefore no longer limited to nearly parallel beams and is possible in many experimental configurations.

(Submitted to Nuclear Instruments and Methods)

^{*)} Visitor from CEN, Saclay, France.

1. INTRODUCTION

An important aspect of the physics experiments with the charged particle beams produced by a high-energy accelerator is the problem of the mass identification of each particle. When the beam momentum p is well defined, the velocity selection, such as obtained for example, by a focusing counter, which may be of the optically corrected type like a DISC^{1,2}), is sufficient to ascertain unambiguously the particle mass m . If $\beta = v/c$ represents the ratio of the velocity of the particle to the speed of light, and as the relativistic factor γ is equal to $(1 - \beta^2)^{-\frac{1}{2}}$, we have $m = p/\beta\gamma$.

Although very selective and efficient, such a discrimination is usually performed simply by focusing the Čerenkov light onto a ring in the plane of an annular diaphragm, set to select the light emitted at an angle θ such that

$$\theta_0 - \frac{\Delta\theta_0}{2} \leq \theta \leq \theta_0 + \frac{\Delta\theta_0}{2} . \quad (1)$$

$\Delta\theta_0$ defines a velocity window of total width $\Delta\beta_0$ around a central velocity β_0 . From the basic Čerenkov relation we have

$$\beta_0 = \frac{1}{n \cos \theta_0} , \quad (2)$$

where n is the refractive index of the radiator, and

$$\Delta\beta_0 = \operatorname{tg} \theta_0 \Delta\theta_0 . \quad (3)$$

At high energies (about 1 GeV) the Čerenkov radiator is usually a gas and, depending on the desired performances, θ can usually take a value between ~ 5 and 150 mrad; $\Delta\theta$ is then in the range 0.05 to 10 mrad. The corresponding diaphragm width, defined by $\Delta\theta_0$ and the equivalent focal length of the detector optics, lies in the range 10^{-2} to 10 mm.

At a given momentum the maximum acceptable value of $\Delta\theta$ is determined by the smallest mass separation required and at high momenta the corresponding $\Delta\beta$ is quite small. It is therefore difficult, for practical reasons, to collect separately the light produced by particles of different masses in a beam and to tag

the particles individually. Moreover the rings of light are centred on a point which is related to the particle direction. Only particles in a well parallel beam can produce Čerenkov rings which do not overlap. Nevertheless with all its difficulties, this method is extremely powerful for the selection of particles of the same type.

The recognition of an acceptable event is usually performed by detecting the coincidence of the pulses produced by photomultipliers distributed around the circumference of the annular diaphragm. A high rejection ratio of 10^4 to 10^6 against unwanted particles can be obtained by this technique, when at least 6, or even 8, photomultipliers are used in high-intensity beams (10^7 particles/second).

However the phase-space acceptance of this type of focusing counter is not very large, as the light emitted by particles making a divergence angle $\tau > \Delta\theta_0/2$ with the detector axis cannot produce a signal in all the phototubes. Indeed it can be shown²⁾ that the acceptance $\mathcal{A} = S \Delta\Omega \Delta p$ of a DISC-type counter is given by:

$$\mathcal{A} = \frac{\pi^2}{48} \Phi^2 p \gamma \operatorname{tg} \theta_0 (\Delta\theta_0)^3, \quad (4)$$

where Φ is the beam diameter accepted by the detector.

If $\Delta\theta_0$ is set to separate two particles of mass M_0 and M_1 at a momentum p then

$$\Delta\theta_0 \leq \frac{|M_1^2 - M_0^2|}{2p^2 \operatorname{tg} \theta_0}. \quad (5)$$

Very often the acceptance \mathcal{A} can just fill, at most, the emittance of a well-collimated beam of particles.

Matching the beam emittance with the detector acceptance is generally obtained at the price of an important restriction on the total particle flux through the counter. Moreover, the tagging is obtained for only one type of particle at a time for a given setting of the index of refraction of the gas radiator.

Motivated by the interest to remove these restrictions, we have studied the possibility to use any focusing counter in a multiplexing mode by replacement of

the usual mechanical diaphragm by an optical system derived from the Spot-Focusing Detector (SFD) principle, as described elsewhere^{3,4}). Such a counter is called here a Multiplexed Čerenkov Counter (MCC) and can be thought of as a multichannel DISC counter.

2. PRINCIPLE OF THE MULTIPLEXED ČERENKOV COUNTER

From what has been explained in Section 1, it appears that a focusing counter can be considered as a one-channel velocity selector set for $\beta_0 \pm \Delta\beta$ and also as a one-channel direction selector set for a maximum beam divergence τ_{\max} . It is clear that one could replace the diaphragm and phototubes by a number of adjacent small photodetectors, covering a certain range in $\Delta\beta$ and having a maximum divergence τ_{\max} . It is then possible by electronics means to select various combinations of photodetectors corresponding to rings associated with various β and τ values. This process corresponds to the recognition of a given pattern of photoelectrons. However, we have to take into consideration the following remarks:

- the number of picture elements (pixels) needed to recognize a circular distribution of photoelectrons is relatively small (6 or 8 in the case of a DISC for example);
- the resolution needed in $\Delta\beta$ requires on the contrary a relatively high density of pixels in the radial direction.

It is then desirable to find a suitable optical set-up which could perform the following functions:

- divide the rings produced into a given number of sectors (8 for example);
- focus the light coming from each sector onto one photodetector element;
- provide the necessary over-all magnification in order to match the resolution in $\Delta\beta$ provided by the focusing optics of the differential or DISC counter to the photodetector size.

In such a case, the photodetectors would be distributed in the final focal plane on linear arrays radially and regularly distributed with respect to the counter

axis. This set-up would be equivalent to a number of differential or DISC counters equal to the number of possible arrangements of photodetectors (one per array for each combination).

The possibility of tagging simultaneously different particles is also a very attractive feature of an MCC.

One of the most important characteristics of an MCC is the fact that essentially all the focusing optics designed for a Čerenkov counter, up to the focal plane where the diaphragm would be placed, remains the same and can be used without modification. A larger number of photodetectors, of course, are needed to collect the data, and the electronic event recognition will be more complex than the single coincidence circuit used with DISC counters.

Such requirements, as shown below, can be met by a toroidal lens simply added to the existing optics of a focusing counter, and it can be shown that such an element can also be used in a spot focusing detector^{3,4)}, in order to extend its use to the case where the target is relatively far from the counter. However, as such an SFD can also be built by modification of an existing focusing counter, we will treat this problem in a general way in the following, and we call MCC, such a modified counter be it designed to be used according to the first mode (radial distribution of photodetectors) or to the second one (SFD like, with a matrix type distribution of photodetectors).

Therefore this article deals exclusively with the discussion and description of the optical parts needed to replace the diaphragm, in order to analyse Čerenkov rings that are of different sizes and are produced by particles at an angle with the counter axis which may be several times larger than the precision $\Delta\theta$ with which the Čerenkov angle must be measured.

3. DESCRIPTION OF THE OPTICAL SYSTEM

It has been shown⁴⁾ that an SFD can be built according to the principles outlined in Ref. 3. In that detector, a special optics containing a doublet of axicon lenses is used to transform the ring image obtained from a focusing optics into a very reduced ring. Such a ring can even become a spot for a given velocity β_0 ,

corresponding to a value γ_0 of the relativistic factor. Essentially this anamorphic optical system operates the optical subtraction of a fixed and constant angle θ_0 to the Čerenkov angle θ . The purpose of this operation is to reduce considerably the size of the matrix of photodetectors which would otherwise be needed to detect particles from an interaction. Although the rings are shrunk the information on the Čerenkov angle is conserved and the resolution $\Delta\beta$ is comparable to what is obtained with DISC counters²⁾.

The direction of the particle is still given by the position of the centre of the ring or spot image. One may, rightly, consider that an SFD is already an MCC designed especially for the analysis of particles emitted from a small target, for example from an interaction target, at a short distance from the counter entrance window.

Here, instead, we describe how one can design, following the same general ideas, an MCC, for the tagging of particles in a nearly parallel beam.

This detector is intended to be installed in a beam line, or spectrometer, before or after a focus T (Fig. 1). The main difference between this MCC and the SFD described in Refs. 3 and 4 is the relative position of the point T (which is a small target in the case of the SFD). Here this point will be at a large distance from the main spherical mirror and on either side along the optical axis, depending whether the beam of particles is converging or diverging when traversing the counter.

Equation (10) of Ref. 3 expresses the condition of spot focusing for a particle with the Čerenkov angle θ_0

$$d(\lambda_2) = \theta_0(2Q - 1) , \quad (6)$$

where the deviation angle $d(\lambda_2)$ for the mean wavelength λ_2 must be equal to the Čerenkov angle multiplied by $(2Q - 1)$.

The parameter Q is a measure of the distance from the principal image plane H of the focusing optics to the target position T, in terms of its focal length F; one has

$$Q = \frac{HT}{2F} . \quad (7)$$

When the optics consists of a single spherical mirror of radius of curvature R , H is on the mirror surface, and $2F = R$. Figures 1 and 2 have been drawn for the case where the presence of the correcting optics does not change the position of the principal plane. The SFD described in Ref. 4 corresponds to the case where T is at the centre of curvature of the mirror, then $Q = 1$ and T is imaged optically on itself at T' .

The axicon deviation must be in this case equal to $+\theta$. The positive sign can be interpreted as a deviation away from the axis. When the distance HT becomes large and negative, as is the case in a slightly converging beam, $2Q - 1$ becomes also large and negative and the deviation $d(\lambda_2)$ must be several times θ . Such a condition is impossible to realize with a single axicon. Theoretically for an exactly parallel beam this deviation must be infinite. But we know that the image produced by the mere association of a single-stage optics and an axicon is not in general well adapted to a detector matrix for two reasons: depending whether the beam of particles is converging on or diverging from the counter, the spot produced is real or virtual, respectively, and in general the magnification of such a system is not adapted to the detector element size. Therefore, a second-stage optics, as in the SFD⁴⁾, is in general needed, producing a real image with the desired magnification; the equivalent focal length EFL of the total system is much larger than the focal length F of the first stage alone. The required angular resolution $\Delta\theta_0$ is such that $P = EFL \cdot \Delta\theta_0$, where P is the pixel size. This second stage may consist of a transfer lens TL which could be physically combined with the axicon. The same principle can apply to an MCC.

The position of this compound system is defined by $T'F_1 = F/(2Q - 1)$, where F_1 is the focal plane of the first-stage optics, or primary focus, T' is the optical image of T in the focusing optics [it has been shown³⁾ that the spot-focusing condition requires that the axicon be placed at T']. In a slightly converging or diverging beam $T'F_1$ is only a small fraction of the focal length of the first-stage optics, and therefore the transfer lens must have a short focal length. The compound system as a consequence must have the properties of a stray bending element,

deviating the rays by

$$d(\lambda_2) = \theta_0(2Q - 1)$$

associated with a strong focusing element of focal length

$$f \sim \frac{F}{2Q - 1}, \quad (8)$$

where Q is large compared to F .

With separate elements this is unrealizable, but as a single combined element they can be replaced by a thin toroidal lens (or mirror).

4. THE TOROIDAL LENS

Only the application to a converging beam of particles will be considered explicitly in what follows. The case of a diverging beam can be treated along similar lines.

A lens element, or a mirror, can be shaped with a toroidal surface. For our purposes we must consider a lens with cross-section as depicted in Fig. 3. In the thin lens approximation the transfer equation for this element is

$$\alpha_2 - \alpha_1 = \frac{h - R_v}{-f} = \frac{-h}{f} + \frac{R_v}{f}. \quad (9)$$

R_v is the radius of the circle, of radius r , which is the locus of the centre of the meridian curve and is equal to the radius of the Villarceau circles⁵⁾ where $r < R_v$, f is the equivalent focal length of a spherical lens with the same curvature $1/r$.

As shown in Fig. 3, f and r are negative quantities. A toroidal mirror could be substituted for this lens with the appropriate modifications. The two terms of expression (9) can be interpreted in the following way.

$-h/f$ is the ray deviation of a thin spherical lens of focal length f .

R_v/f is a constant deviation, the same as would be produced by an axicon of bending angle $d(\lambda_2) = R_v/f$.

Therefore a toroidal lens of this shape -- in the thin lens approximation -- is equivalent to the combination of an axicon with a spherical lens, both of very strong power, in fact unrealizable with separate elements because both $-h/f$ and R_v/f can easily be larger than 1.

This useful cancellation of extreme shapes for these two elements, and their reduction to a thin lens when combined, is valid only for an annular region of the lens of mean radius R_v , but it can be seen by ray tracing that only this part of the lens or mirror is needed to collect all the Čerenkov light rays focused as rings in the primary focal plane for large values of Q .

A toroidal mirror can perform the same optical function without introducing chromatism, a consideration of some importance when the focusing optics is already well corrected chromatically as in DISC-type counters, but it may be undesirable because of the complication introduced by the folding of the light path.

5. THE MULTIPLEXING OPTICS

A toroidal lens or mirror is the basic element to transform any focusing-type Čerenkov counter into an MCC. An SFD is indeed a particular MCC and can, from what has been shown above, be constructed by adding to a focusing optics producing the usual ring images, a toroidal lens transforming these images into a real spot for $\gamma = \gamma_0$ or small rings for $\gamma \neq \gamma_0$ in the final focal plane. A matrix of small photo-detectors can be used to decode the new pattern produced, measure γ , and obtain the particle direction from τ and ϕ .

The spot focusing condition will be detected through pulse-height selection, and the small circles will be recognized by coincidence selection among different pixels of the matrix. This method can provide a trigger for the very fast acquisition of the particles having $\gamma = \gamma_0$, independently of their divergence angles τ and ψ . However this set-up is not necessarily the best for all the cases of beam particle identification that may occur.

We may want instead to analyse the pattern in a uniform way, relying on multiple coincidences in a manner similar to the one generally applied to DISC counters, where the rule is to require octuple coincidences for the selection of an event, with a very high degree of reliability. This mode of data acquisition can be obtained in the following way with an MCC. The image ring produced by the first stage optics (differential or DISC counter) is projected at infinity by a toroidal

lens. It is then possible with a series of eight spherical lenses of focal length F_L , each of them intercepting 1/8 of this annular parallel beam to focus it onto a point for $\gamma = \gamma_0$. In this way the light from a spot is split equally among eight photodetectors and octuple coincidences can be recorded. When $\gamma \neq \gamma_0$ the Čerenkov light seems to come from rings of small angular size at infinity, and will be imaged by the lenses on the eight linear arrays as small arcs of a circle. The pixel width must be large enough to accommodate for the radial extension of this arc, i.e.

$$\text{Pixel width} \geq \left(1 - \cos \frac{\pi}{8}\right) \cdot \text{EFL} \cdot \Delta\theta = \frac{0.076}{2 \operatorname{tg} \theta} \left| \frac{1}{\gamma^2} - \frac{1}{\gamma_0^2} \right|. \quad (10)$$

In this formula EFL is the equivalent focal length of the system as a whole. Figures 4a to 4g show examples of the arrays of photodetectors that could be used and the pattern of pixels illuminated for different combinations of γ , τ and ψ . It must be understood that the number of arrays may be different from eight. This value is convenient in most cases.

One must point out an important difference between an MCC fitted with split radial arrays of photodetectors and an SFD with a single matrix. The ambiguity on the sign of $\theta - \theta_0$ observed in an SFD⁴⁾ and the double solution for the value of γ , do not appear in a split-matrix MCC.

The eight lenses besides their image-focusing properties offer the possibility of being the windows of the pressure vessel, with the advantage of a reduction in the number of optical elements and a better light transmission. The optical system formed by the toroidal lens and the imaging lenses associated with the matrix arrays is essentially what may be called an electronic diaphragm. The selection of a particle with a Čerenkov angle θ , a divergence angle τ and an azimuth angle ψ , is obtained from a multiple coincidence, like in a focusing counter with a mechanical diaphragm, between photodetectors selected each in a different array according to a predetermined truth table (Fig. 4). The number of acceptable combinations is a measure of the multiplexing factor.

One may also think of this optical system as a special anamorphic lens, which has the properties of magnifying radially the variation of the Čerenkov

angle $\Delta\theta$, by making the EFL of the system quite large, and of contracting azimuthally the final ring image into very small segments (indeed a spot for γ_0), whose light can be effectively collected by miniature photomultipliers, like the R760 of 16 mm outside dimension, without the need for any optical light guide.

Figure 4 shows that linear arrays with square pixels can cover a sizeable range of $\Delta\theta$, τ , and ψ .

6. DESIGN OF THE MCC OPTICS

The necessary relations needed for the design of an MCC can be deduced from the formula derived for an SFD³⁾. The same notations with some additions will be used, and the reader is referred to Ref. 3 for the derivation of the formulae.

- i) The equivalent focal length of a spherical lens or mirror having the radius of curvature r of the meridian of the torus is f .
- ii) R_v is the radius of the circle, which is the locus of the centre of the meridian curve, a circle of radius r .
- iii) F is the focal length of the original counter to which the MCC optics is fitted.

The particle beam waist is at the position T , at a distance $HT = 2QF$ from the principal plane of the original counter optics, and its image is at T' , at a distance

$$HT' = \frac{2Q \cdot F}{2Q - 1} . \quad (11)$$

The distance between the original counter primary focus F_1 and the point T' (where according to the SFD theory the toroidal lens must be placed to achieve spot focusing) is

$$F_1T' = \frac{F}{2Q - 1} . \quad (12)$$

The final focus of the MCC is at position F_2 on the optical axis. The magnification between F_1 and F_2 is G . The toroidal lens can be used alone (case 1) and in this case the MCC produces a focalized pattern exactly as for an SFD, or we can add to this optical system a set of slicing lenses of focal length F_L as described

above (case 2). In this last case the intermediate image of the toroidal lenses is at infinity.

The equivalent focal length EFL is therefore

$$\text{EFL} = F \cdot G, \text{ with } G = \frac{T'F_2}{T'F_1} \quad (13)$$

and the radial displacement ΔR of the spot or ring image as a function of $\Delta\theta$ will be

$$\Delta R = \text{EFL} \cdot \Delta\theta \quad (14)$$

In the first case (Fig. 1) the spot focalization on the optical axis is obtained when the following conditions are realized for the toroidal lens

$$f = \frac{F}{2Q - 1} \frac{G}{(1 + G)} \quad (15)$$

$$R_v = \frac{G \cdot F \cdot \theta}{1 + G} \quad (16)$$

with

$$F_1 T' = \frac{F}{2Q - 1} = f \frac{1 + G}{G} \quad (17)$$

In the second case (Fig. 2) the toroidal lens and the focusing optics form an "afocal system", i.e. the spot image is at infinity and the magnification G is infinite.

The toroidal lens prescriptions are the following:

$$f = \frac{F}{2Q - 1} \quad (18)$$

$$R_v = F \cdot \theta \quad (19)$$

This last relation shows that the radius R_v of the centre of the meridian generating the toroidal lens is equal to the Čerenkov ring radius focalized by the optics.

The position of the toroidal lens is given by

$$T'F_1 = f \quad (20)$$

The final foci are in the focal plane of the slicing lenses

$$T'F_2 = F_L . \quad (21)$$

The equivalent focal length of the MCC is

$$EFL = F \cdot \frac{F_L}{f} . \quad (22)$$

6.1 Shape of the spot or ring image

When the particle detected does not cross the optical axis at the point T but at a distance δ from this point, the spot or the ring image is distorted. From formula (9) of Ref. 3 the Cartesian coordinates of the image, given by the MCC in the final focal plane F_2 , can be derived easily for the first case (spot-focusing mode, according to Fig. 1). When slicing lenses are used as in the second case (Fig. 2), the pattern is cut and each portion displaced from the optical axis. The trivial appropriate translations must be applied in this case.

The equations of the image produced in the image plane of a system consisting of a spherical mirror and an axicon placed at the optical image T' of a target T in the mirror are³⁾ (see Fig. 5)

$$\begin{aligned} X &= F \left[\left(\theta - \frac{d}{2Q-1} \right) \cos \omega - \frac{\delta d}{2F\theta_0(Q-W)(2Q-1)} \sin \omega \cos \omega + \tau \cos \psi \right] \\ Y &= F \left[\left(\theta - \frac{d}{2Q-1} \right) \sin \omega + \frac{\delta d}{2F\theta_0(Q-W)(2Q-1)} \cos^2 \omega + \tau \sin \psi \right] \end{aligned} \quad (23)$$

where

ω is the azimuth angle of a light ray emitted at a distance $2WF$ from the mirror;

d is the bending angle of the axicon, which, according to Eq. (8) is equal to $\theta_0(2Q-1)$;

δ is the impact parameter of the trajectory (distance to the optical axis);

τ and ψ are the divergence and azimuth angle of the trajectory, respectively.

By writing $\Delta\theta = \theta - \theta_0$, these equations can then be rewritten

$$\begin{aligned} X &= F \left[\Delta\theta \cos \omega - \frac{\delta}{2F} \frac{\sin \omega \cos \omega}{(Q - W)} + \tau \cos \psi \right] \\ Y &= F \left[\Delta\theta \sin \omega - \frac{\delta}{2F} \frac{\cos^2 \omega}{(Q - W)} + \tau \sin \psi \right]. \end{aligned} \quad (23')$$

To such a system is added in T' a thin spherical lens of focal length f which magnifies the image by a factor G_0 . The combination of the axicon and the lens is equivalent to a torus, as seen above, and the EFL of the complete system is

$$EFL = F \cdot G$$

and

$$G = T'F_2 / T'F_1, \quad (24)$$

where F_2 is the position of the final image plane. The final image is then described by

$$\begin{aligned} X_F &= EFL \left[\Delta\theta \cos \omega - \frac{\delta}{2F} \frac{\sin \omega \cos \omega}{(Q - W)} + \tau \cos \psi \right] \\ Y_F &= EFL \left[\Delta\theta \sin \omega + \frac{\delta}{2F} \frac{\cos^2 \omega}{(Q - W)} + \tau \sin \psi \right]. \end{aligned} \quad (25)$$

For each value of W the photons are focalized along a curve described by Eq. (25).

The SFD described in Refs. 3 and 4 is designed with $Q = 1$, and W can vary from 0 to 0.8. For this detector the range of $(Q - W)$ is not negligible and the final image is obtained by integration over this range. The conditions are different in an MCC; Q may take values between 5 and 20, as the beam waist is supposed to be far from the detector, and the range of variation of W is about 0 to 0.5 as the radiator length is $\sim F$.

Therefore the effect of the variation of W can be neglected and the image is limited to a curve described by the following equations

$$\begin{aligned} \frac{X_F}{EFL} &= \tau \cos \psi + \Delta\theta \cos \omega - \frac{\delta}{4F} \frac{\sin 2\omega}{Q} \\ \frac{Y_F}{EFL} &= \tau \sin \psi + \Delta\theta \sin \omega + \frac{\delta}{4F} \frac{\cos 2\omega}{Q} + \frac{\delta}{4F \cdot Q}. \end{aligned} \quad (26)$$

The different terms of these equations represent angular displacement and can be easily interpreted (Fig. 6).

When $\delta \sim 0$, Eqs. (26) represent a circle at infinity centred on the particle trajectory and of semi-angle $\Delta\theta$. For the spot-focusing condition $\Delta\theta = \theta = \theta_0 = 0$, we have a spot in the focal plane and a small ring when the condition is not realized, centred on the intersection of the particle trajectory with a plane at a distance EFL from T. In the general case, Eqs. (26) represent the equation of a Pascal Limaçon at infinity, i.e. an epicycloidal curve with one loop. The $\delta/4F \cdot Q$ is a displacement along the Y axis only, because the system of coordinates has been chosen¹⁾ in such a way that the intersection of the particle trajectory with the plane at T is at a distance δ from T and in the YOZ plane.

In some cases this Limaçon certainly departs too much from a circle, but the approximation may still be considered valid, when the loop degenerates into a cusp and the curve becomes a cardioid. This is realized when

$$\frac{\Delta\theta}{2} \geq \frac{\delta}{4F(Q - W)}, \quad (27)$$

$$\delta \leq 2F(Q - W)\Delta\theta. \quad (28)$$

An important consideration not to be overlooked is the light flux distribution along the image, which is not uniform when the curve is no longer a circle, only $\Delta N/\Delta W$ is constant (N is the number of photons).

6.2 Effect of the impact parameter δ on the MCC resolution

In general, the impact parameter δ is not known, unless some hodoscope or multiwire proportional chambers are used to define the particle trajectory near the point T. If δ is known, the curve can be fitted with the appropriate epicycloid and $\Delta\theta$ obtained without errors caused by δ .

When this is not possible some indetermination of $\Delta\theta$ is introduced by the impact parameter δ . Indeed it is possible to have an exact circle for two conditions: one when $\Delta\theta = 0$, $\delta \neq 0$, and the radius = $(\delta \cdot \text{EFL})/4F(Q - W)$, and the

other when $\Delta\theta \neq 0$, $\delta = 0$, and the radius = $\Delta\theta \cdot \text{EFL}$. This can easily be seen from inspection of Eqs. (25). The ambiguity amounts to interpreting the circle in the first case as corresponding to $\Delta\theta = \delta/4F(Q - W)$ instead of $\Delta\theta = 0$.

In order to appreciate the magnitude of the errors in the $\Delta\theta$ measurement caused by δ , a numerical example may be informative.

We take as focusing optics the parameters of the FNAL-CERN DISC counter²⁾

$$\theta = 25 \times 10^{-3}$$

$$F = 4500 \text{ mm}$$

$$\text{HT} = 2Q \cdot f = 4500 \text{ mm}$$

$$Q = 5$$

$$\Delta\theta = \frac{\delta}{2 \times 4500 \times 5.5} = 2 \times 10^{-5} \times \delta_{\text{mm}} \text{ radian}$$

$$\begin{aligned} \frac{\Delta\beta}{\beta} &= \text{tg } \theta \Delta\theta = 25 \times 10^{-3} \times 2 \times 10^{-5} \delta_{\text{mm}} = 50 \times 10^{-8} \\ &= 5 \times 10^{-7} \delta_{\text{mm}} \end{aligned}$$

The ultimate resolution of this DISC optics is 4×10^{-7} , which is about the diffraction limit; therefore to degrade its velocity resolution by a factor of 10, and the maximum momentum at which it will separate two particles in an identical way by the factor $\sqrt{10} = 3.3$, the waist radius must be as large as 8 mm. The usual beam waist can be about a third of that in a well-focused beam at the CERN SPS or Fermilab. The distortion of the ring image will not have an important effect on the resolution of an MCC.

6.3 Feasibility of the toroidal lens or mirror

The toroidal lens or mirror is the essential optical element of an MCC. The practical interest of this new Čerenkov detector is clearly related to the possibility of producing such a lens (the mirror is obtained by vacuum aluminization of the lens) with the required accuracy.

Some geometrical arguments show that such lenses can easily be generated and diamond-cut on a single milling machine, and only polishing is then needed to finish them.

A torus can be cut by a bitangent plane along a quartic curve which degenerates into two circles of the same radius R_V as the circle described by the rotation around the torus axis of the meridian circle of radius r ⁵⁾.

Therefore the rotation of one of these two circles around the same axis generates the torus. Any surface parallel to a torus is a torus. A few examples of such toroidal lenses have been made at CERN. This is possible only when the Villarceau circles are real, this implying the condition that $r < R_V$.

Starting from a plane parallel plate of glass set on a rotating table, the toroidal surface was generated with a bell-shaped diamond guiding wheel of mean radius $R_V = 135$ mm, with a round edge of radius $\rho = 2.5$ mm. The axis of the guiding wheel was inclined at an angle α such that $\arcsin \alpha = (r - \rho)/R_V$, and offset from the axis of the rotating table by a distance r .

In this manner the contact of the cutting edge with the glass occurs along about half the perimeter of the guiding wheel, producing a very clean surface nearly free of striations, ready to be polished. In our feasibility test we have chosen to use very fast felt polishing with cerium oxide to finish the lens. As expected, some orange peel defect was evident, particularly with laser illumination. This can certainly be avoided with a more careful pitch polishing, the usual technique for the production of precision lenses.

One of these lenses was illuminated on the optical bench with light coming from a simulated Čerenkov ring. For this purpose the axicon-mirror combination of the SFD described in Ref. 4 was used as a simulator.

In the SFD this optical system transforms a Čerenkov ring produced by a main mirror into a spot; therefore, by using this system in the reverse mode with a punctual light source obtained by a HeNe laser and a microscope objective at the place of the spot, the light after transmission and reflection in the axicon-mirror combination is focused into a real ring. The pattern described by Eqs. (26) and the distortions shown in Fig. 6 were observed on a screen in the plane of the photodetectors, confirming the previous calculations.

Slicing lenses were also tested with the toroidal lenses, giving a spot at infinity, with the expected results.

An MCC designed to identify the particles emerging from a target would require, as shown by formulae (14) and (19), a positive toroidal lens instead of a negative one, which is the only type that can be machined with the previously described method. However, a positive lens can be replaced by a toroidal positive mirror obtained by aluminizing a negative toroidal lens and using it as a front surface mirror. An MCC can therefore be built to be used with converging or diverging beams.

7. CONCLUSIONS

We have shown that by the use of a toroidal lens, which is easily manufactured, it is possible to use a spot-focusing detector after an interaction target or in beam when the waist or the target are relatively far from the counter. We have also shown that it is possible to modify a differential or DISC counter in order to make it a multichannel detector by replacing its usual mechanical diaphragm and photomultipliers by an opto-electronic system where the light detection is done by a set of linear photodetector arrays distributed radially in the final image plane. The angular acceptance and velocity range of such detectors can be increased considerably without modification of their velocity resolution and with only a modest increase in the number of photodetectors. With only 40 pixels instead of 8 as in a conventional DISC, the MCC with the detectors shown in Fig. 4 will have 85 times the acceptance of the equivalent DISC. The possibility of using a focusing counter, so far restricted to parallel beams, in converging or diverging beams brings about much flexibility in the design of the set-up of an experiment. An MCC, as well as an SFD, opens up the new possibility to tag many particles emitted at the same time, or within the resolving time of the photodetectors.

For example, the tagging of the kaons in an intense focused beam containing pions and kaons can easily be accomplished. The index of refraction is adjusted to produce spot focusing for the kaons. Only these particles will create bright spots of Čerenkov light on the photodetector matrix, which can be detected among

the light of the pions spread over a large number of pixels. At the same time the direction of the kaons is obtained from the position of the spot on the detector matrix.

The MCC technique can be applied to low-energy particles with a liquid radiator. Figure 7 gives an outline of a possible configuration of such a counter which will be very compact. Analysis of the spot displayed on the main mirror surface could be made with the help of optical light guides conveying the Čerenkov light to externally placed photodetectors.

Acknowledgement

The precise glass grinding done by M. Carminati, M. Gasparini and C. Nichols of the optical shop is deeply appreciated.

REFERENCES

- 1) M. Benot, J. Litt and R. Meunier, Nucl. Instr. and Meth. 105 (1972) 431.
- 2) J. Litt and R. Meunier, Annu. Rev. Nucl. Sci. 23 (1973) 1-43.
- 3) M. Benot, J.M. Howie, J. Litt and R. Meunier, Nucl. Instr. and Meth. 111 (1973) 397-412.
- 4) M. Benot, J.C. Bertrand, A. Maurer and R. Meunier, A spot-focusing detector, to be submitted to Nucl. Instr. and Meth.
- 5) A. Yvon Villarceau, Discovery, in 1848, of a third system of circular sections of a torus, Communication to the Académie des Sciences, Paris, 1867.

Figure captions

- Fig. 1 : Optical system of a spot-focusing Čerenkov counter using a toroidal lens. For the case of a diverging beam, the negative toroidal lens must be replaced by a positive one.
- Fig. 2 : Optical system of a multiplexed Čerenkov counter. A set of spherical lenses split and display the pattern on radial arrays of photodetectors.
- Fig. 3 : Negative toroidal lens.
- Fig. 4 : Front view of eight radial arrays of photodetectors, each one containing five pixels. A larger number of pixels could be used in an actual detector. The pattern of the pixels receiving Čerenkov light is depicted for different combinations of $\Delta\theta$, τ , and ψ . $\Delta\theta$ and τ are measured in units of the pixel size P divided by the equivalent focal length EFL. The number of different patterns in this simple arrangement corresponds to 85 combinations of $\Delta\theta$, τ , and ψ . The acceptance of this MCC is 85 times larger than for a DISC with the same resolution.
- Fig. 5 : Principle of a spot-focusing detector consisting of a spherical mirror and an axicon placed at the optical image T' of a target at T in the mirror.
- Fig. 6 : Focalized line of Čerenkov light for an extreme case where the ring is strongly distorted. In the actual case the ring will not show a cusp but only a bump.
- Fig. 7 : Possible design of an MCC for low-energy particles, with a liquid radiator.

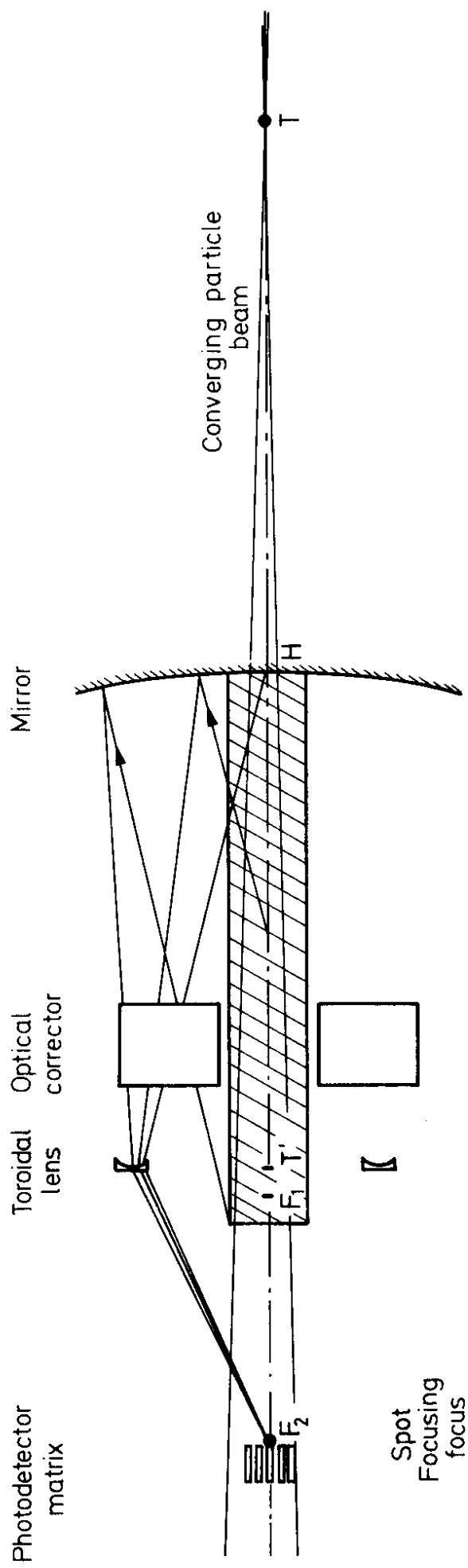


Fig. 1

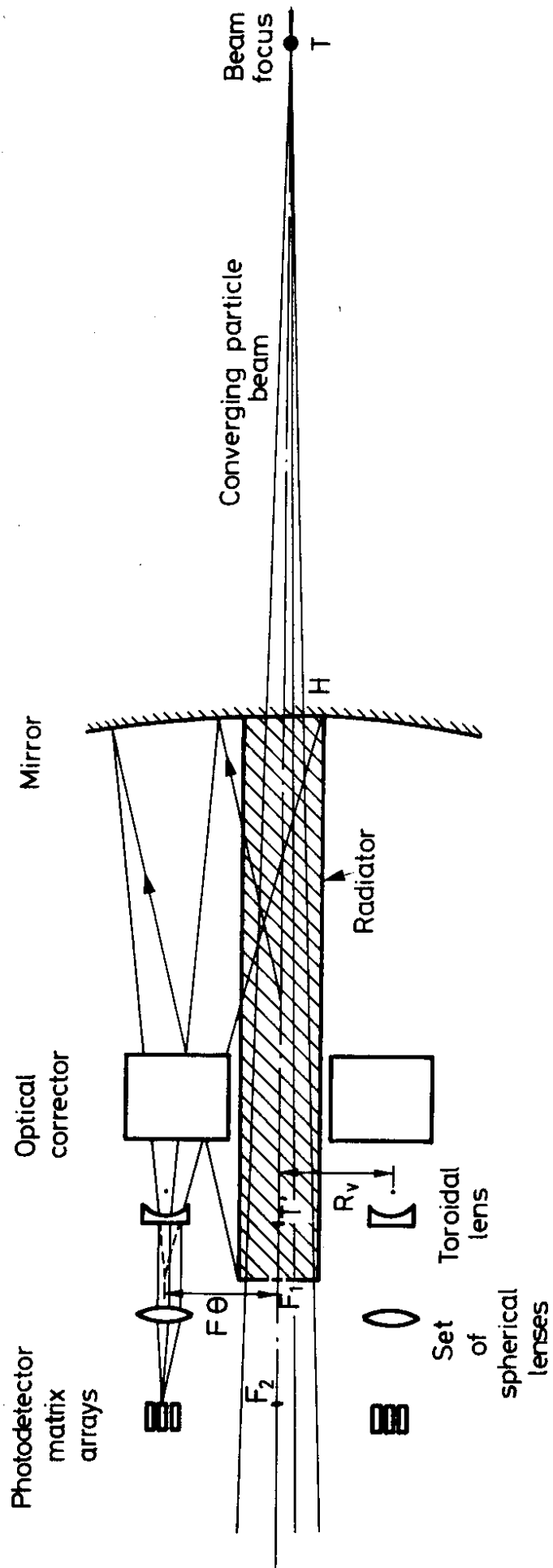


Fig. 2

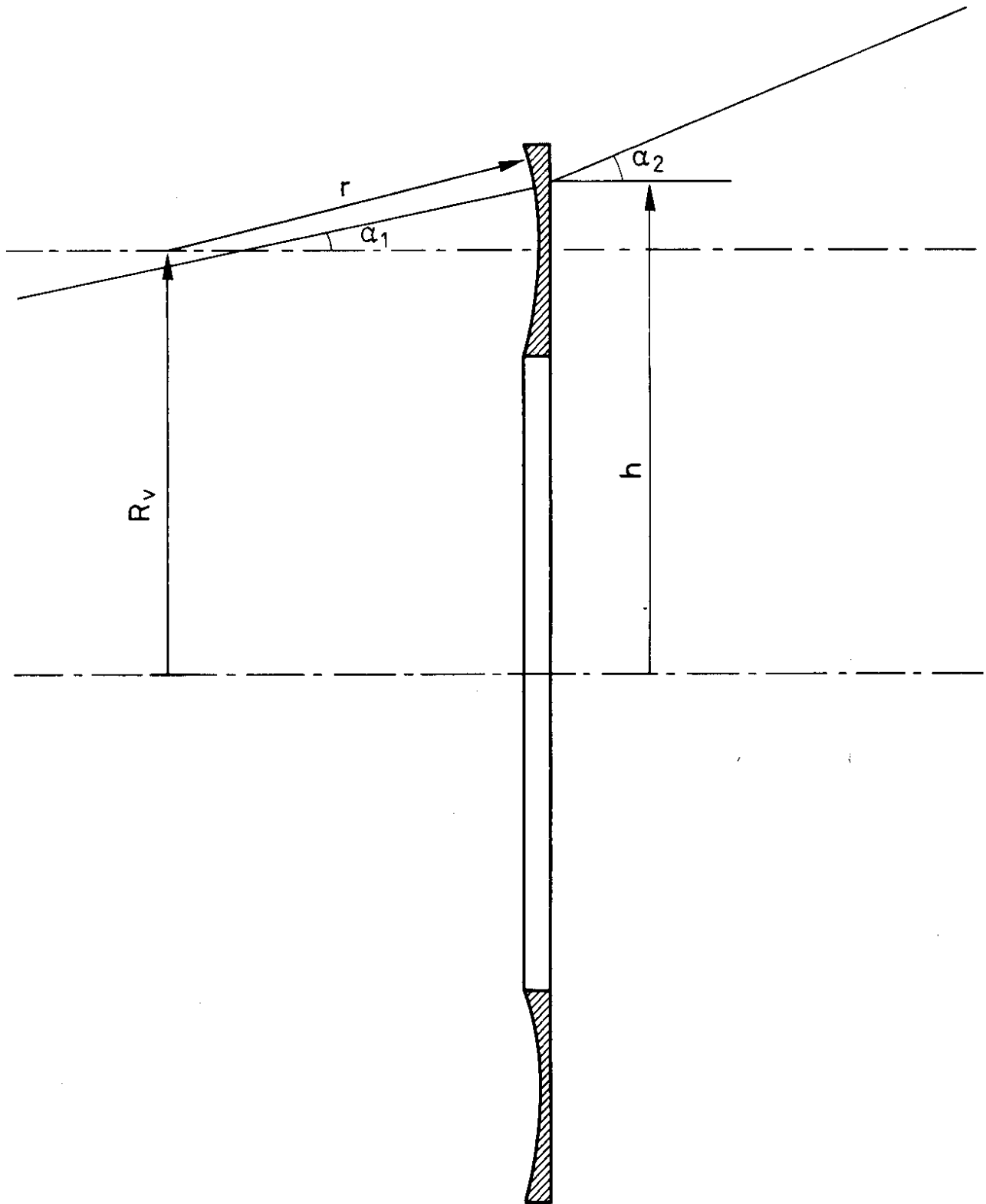


Fig. 3

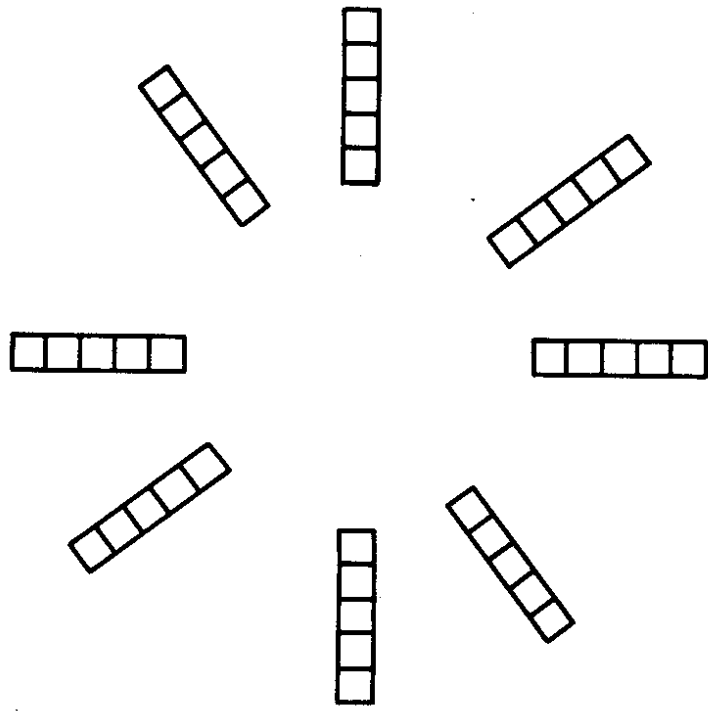


Fig. 4a

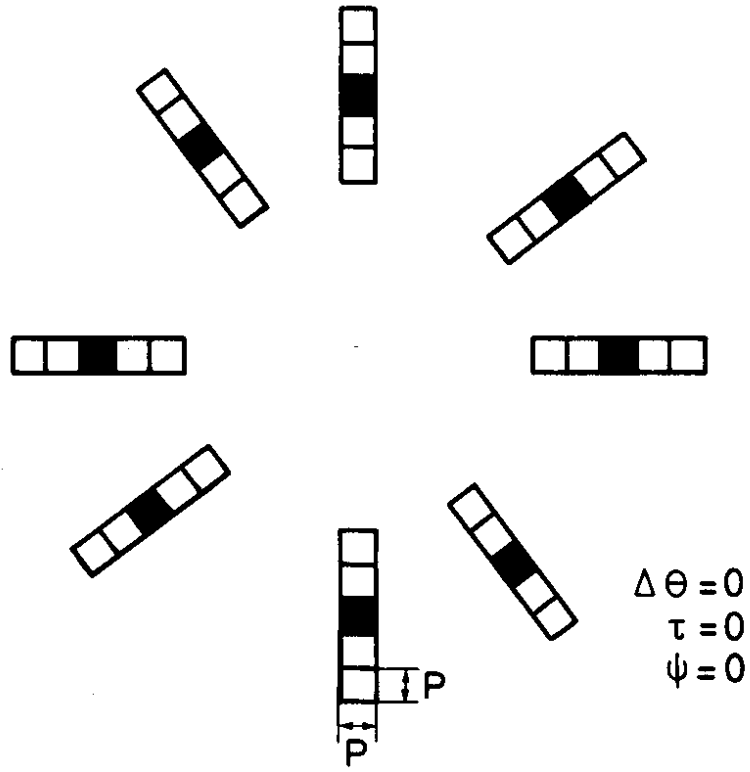


Fig. 4b

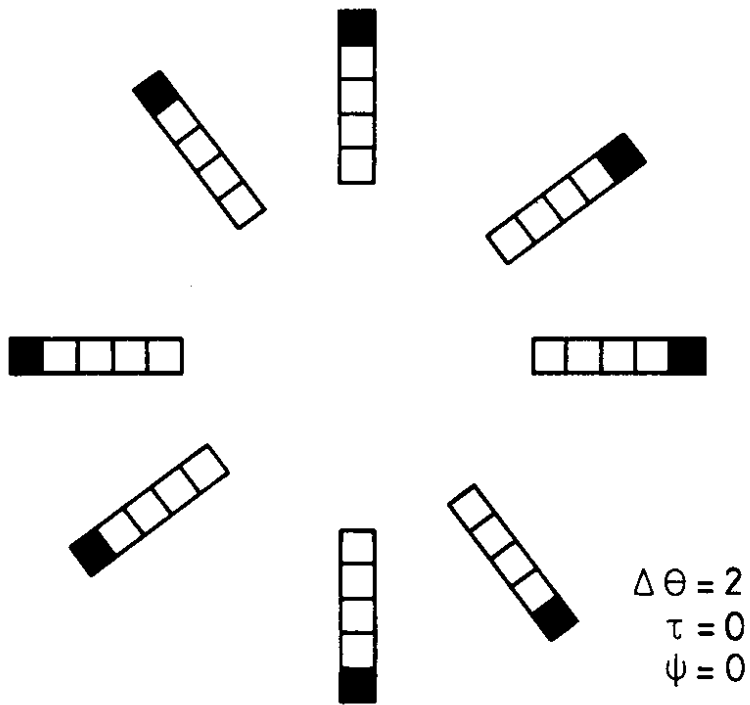


Fig. 4c

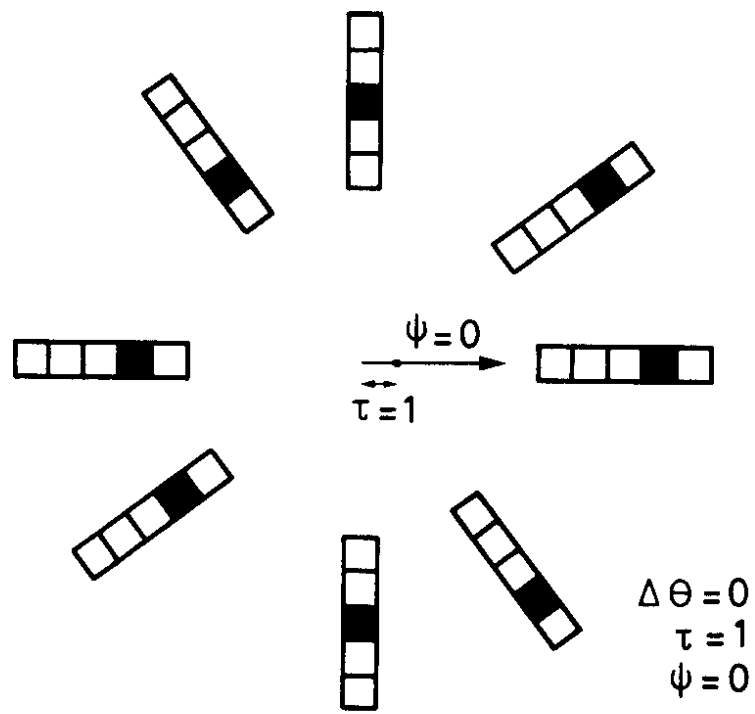


Fig. 4d

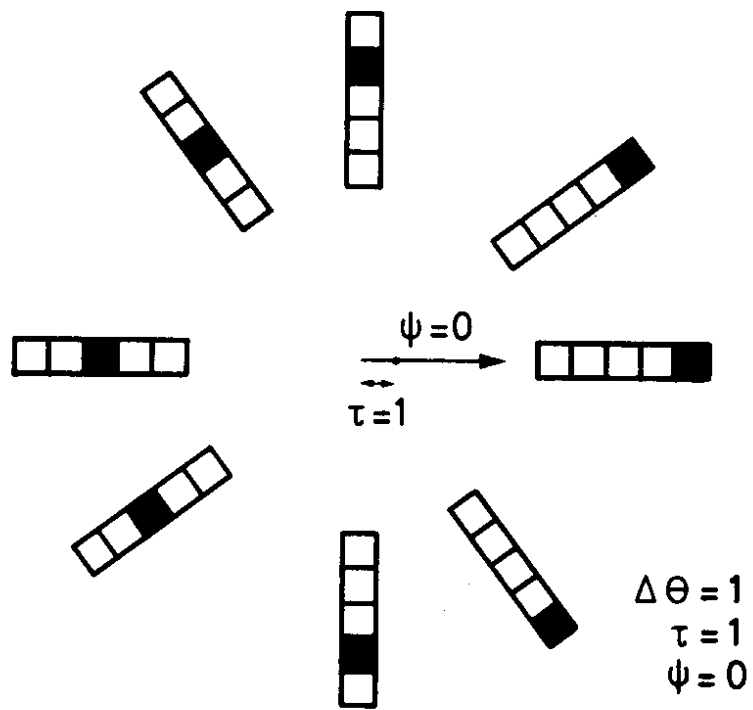


Fig. 4e

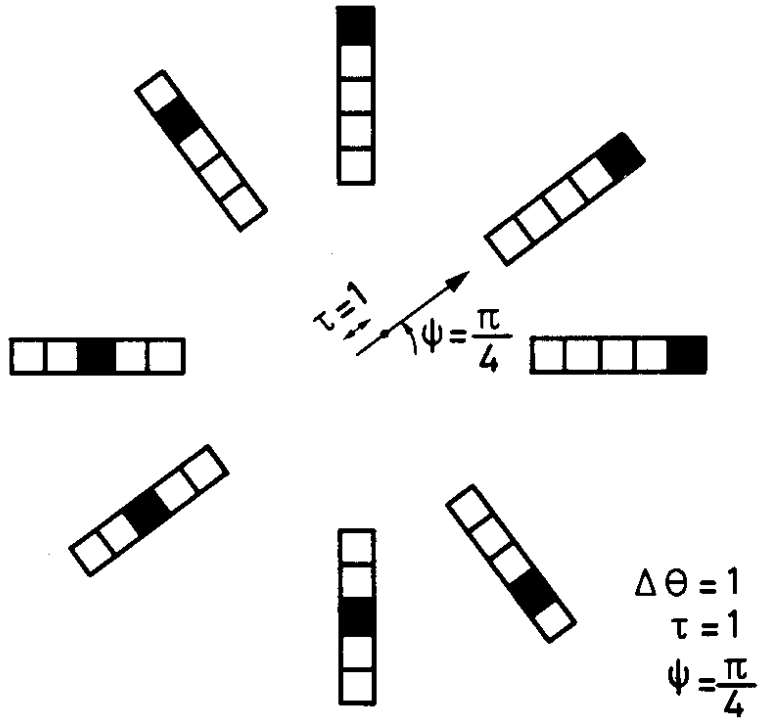


Fig. 4f

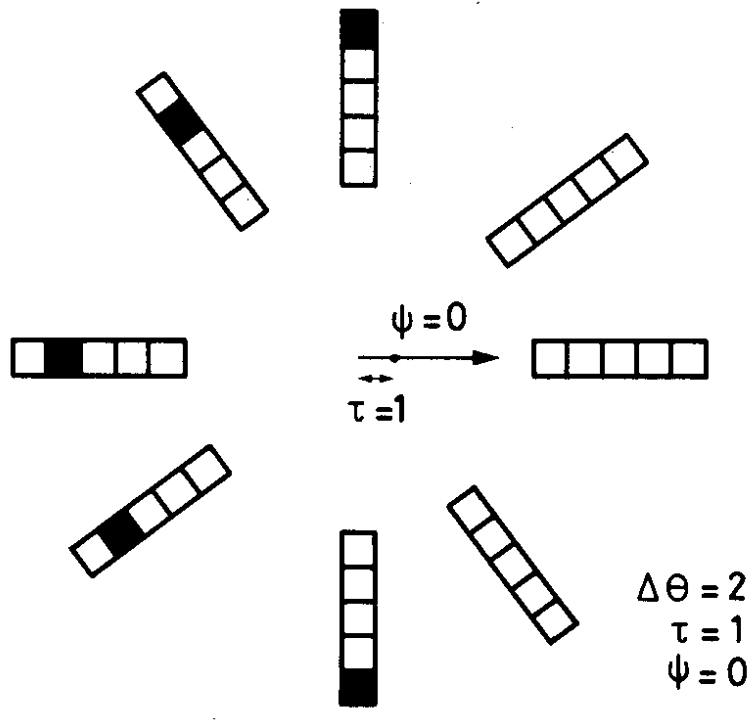


Fig. 4g

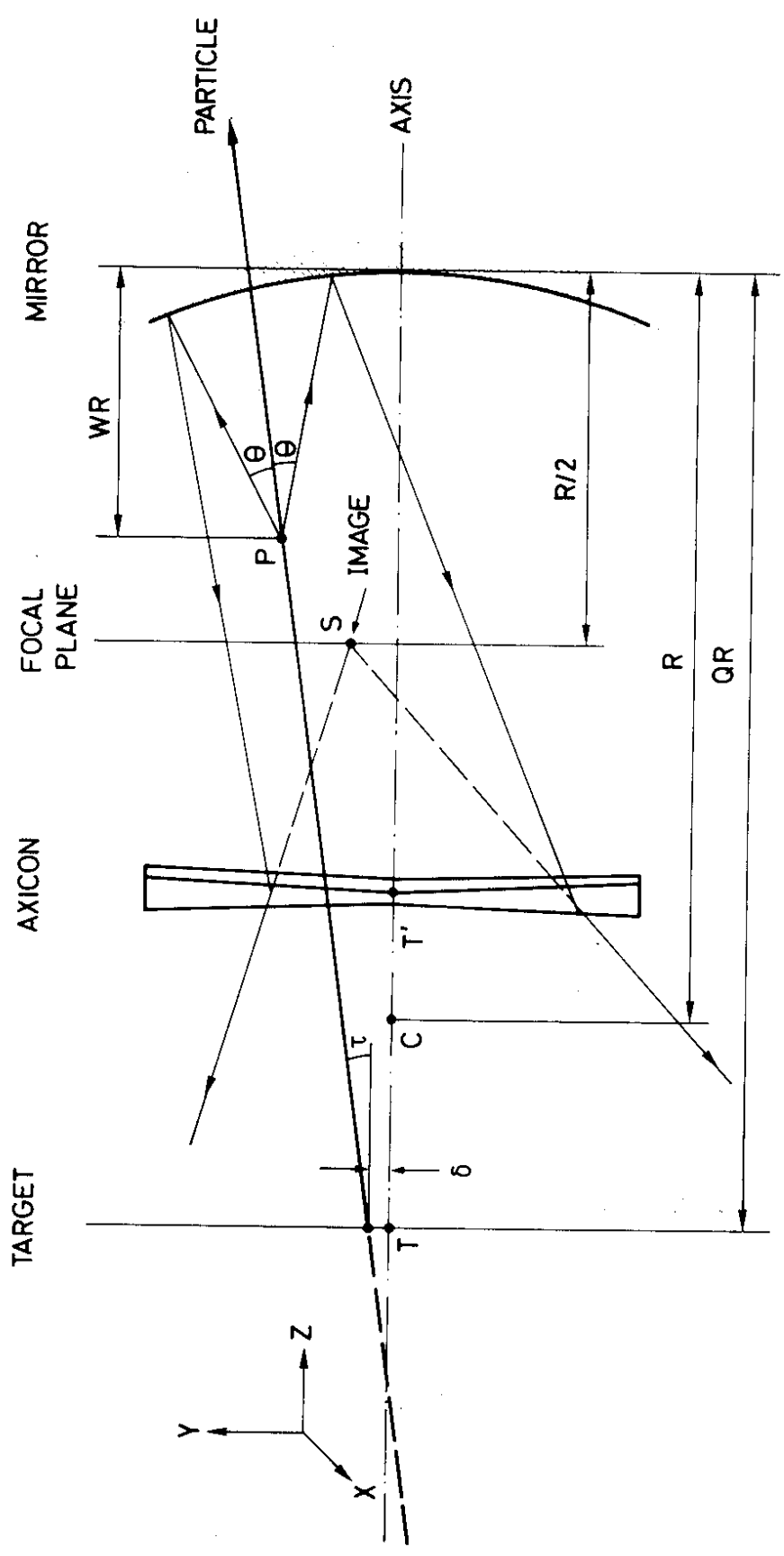


Fig. 5

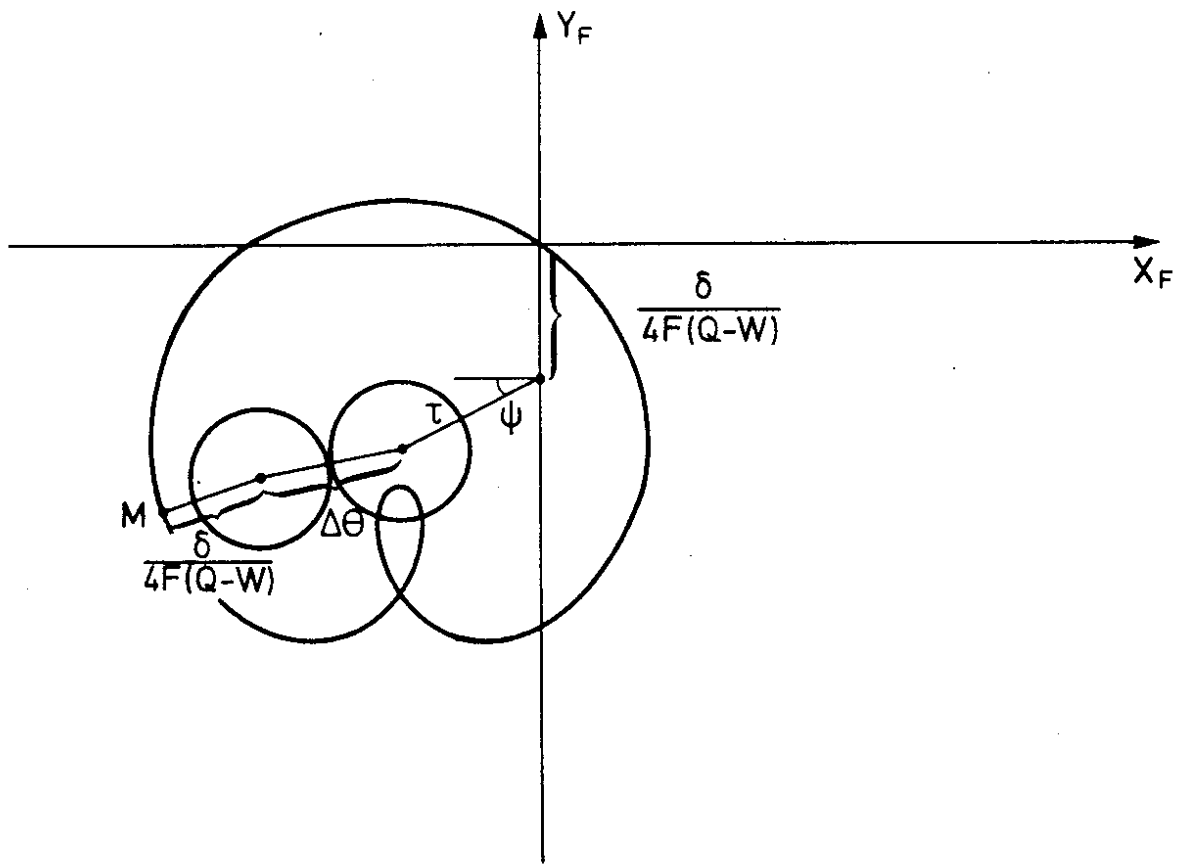


Fig. 6

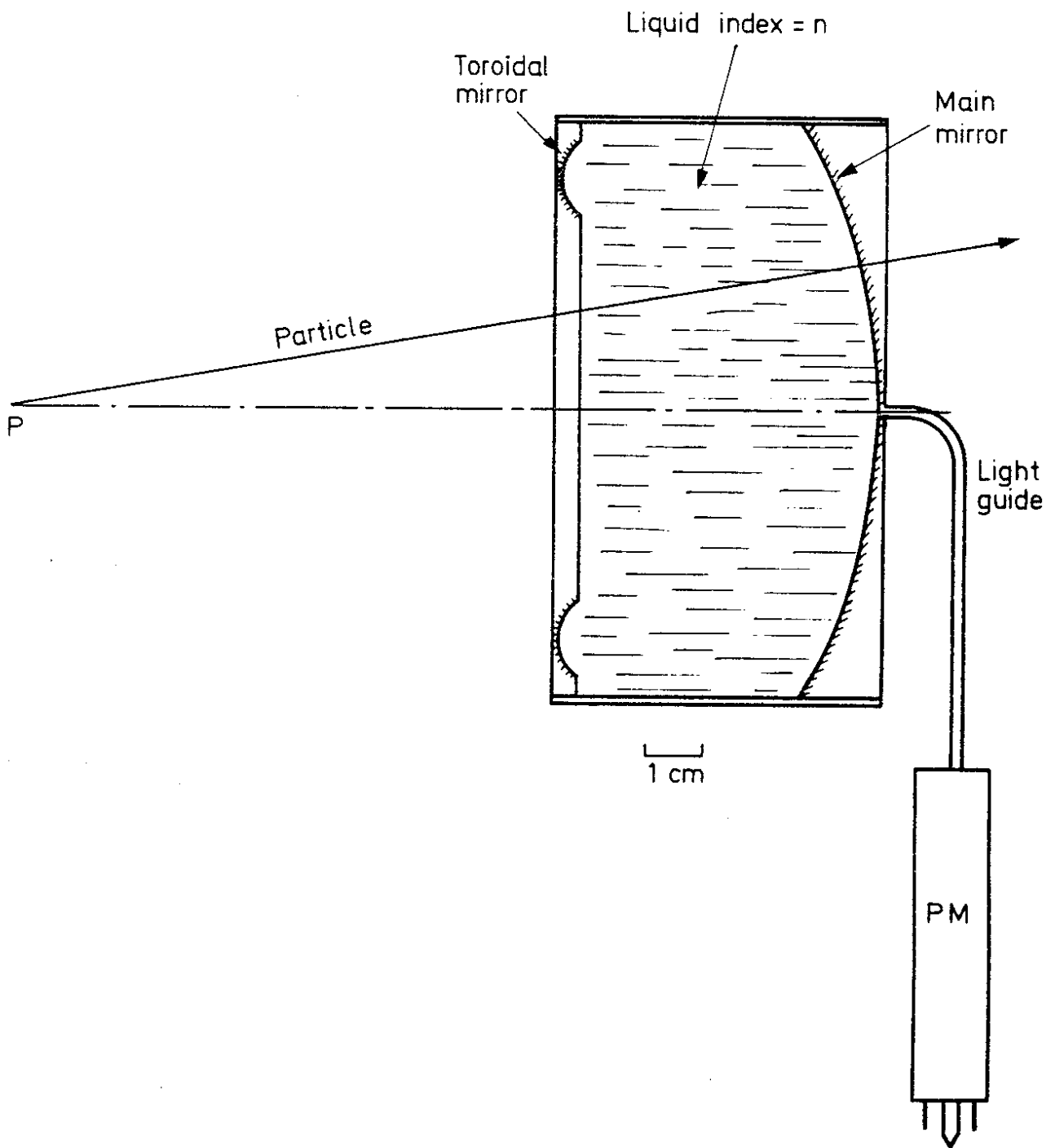


Fig. 7.